



Pore former induced porosity in LSM/CGO cathodes for electrochemical cells for flue gas purification

Skovgaard, M.; Andersen, Kjeld Bøhm; Kammer Hansen, Kent

Published in:
Ceramics International

Link to article, DOI:
[10.1016/j.ceramint.2011.09.052](https://doi.org/10.1016/j.ceramint.2011.09.052)

Publication date:
2012

[Link back to DTU Orbit](#)

Citation (APA):
Skovgaard, M., Andersen, K. B., & Kammer Hansen, K. (2012). Pore former induced porosity in LSM/CGO cathodes for electrochemical cells for flue gas purification. *Ceramics International*, 38(2), 1751-1754.
<https://doi.org/10.1016/j.ceramint.2011.09.052>

General rights

Copyright and moral rights for the publications made accessible in the public portal are retained by the authors and/or other copyright owners and it is a condition of accessing publications that users recognise and abide by the legal requirements associated with these rights.

- Users may download and print one copy of any publication from the public portal for the purpose of private study or research.
- You may not further distribute the material or use it for any profit-making activity or commercial gain
- You may freely distribute the URL identifying the publication in the public portal

If you believe that this document breaches copyright please contact us providing details, and we will remove access to the work immediately and investigate your claim.

Pore former induced porosity in LSM/CGO cathodes for electrochemical cells for flue gas purification

M. Skovgaard, K.B. Andersen, K.K. Hansen*

Fuel Cells and Solid State Chemistry Division, Risø National Laboratory for Sustainable Energy, Technical University of Denmark, Frederiksborgvej 399, 4000 Roskilde, Denmark

*Phone: +45 4677 5835, Fax: +45 4677 5858, e-mail address: kkha@risoe.dtu.dk

Abstract

In this study the effect of the characteristics of polymethyl methacrylate (PMMA) poreformers on the porosity, pore size distribution and the air flow through the prepared Lanthanum Strontium Manganate/Gadolinium-doped Cerium oxide (LSM/CGO) cathodes was investigated. Porous cathodes were obtained and the highest porosity measured was 46.4 % with an average pore diameter of 0.98 μm . The air flow through this cathode was measured to 5.8 ml/(min*mm²). Also the effect of exposure time to the solvent was tested for the most promising PMMA pore former and it was found that the average pore diameter decreases as a result of elongated exposure. Also prolong milling of the LSM powder was found to decrease the porosity of the final cathode and milling time should be highly controlled in order to obtain as porous cathodes as possible.

Keywords: Tape casting, porosities, electrodes, materials preparations

Introduction

Exhaust from diesel engines contains nitrogen oxides, which are formed as a side product from N₂ and O₂ at high temperatures. NO_x are known to have negative effects on the human health and to cause environmental problems such as acid rain, high local ozone concentrations [1, 2]. Exhaust from diesel engines also contains soot particles, which is known to be carcinogenic [3].

For these reasons great efforts have been made to remove NO_x and soot from the exhaust stream of diesel engines. One approach is to electrochemically reduce NO by the use of an electrochemical cell. This type of cell is composed of a porous electrolyte layer between two porous electrodes. During the catalytic process NO is reduced at the cathode under formation of nitrogen and oxygen ions. The oxygen ions are then transported through the electrolyte to the anode, where they react with the soot to form CO₂ [4]. In order to reduce the pressure drop across the cell and capture the soot particles the porosity of the different layers of the cell should be controlled carefully.

Perovskite type oxides are mixed oxides with the composition ABO_3 or A_2BO_4 . These metal oxides have the advantages of being stable at high temperatures, being cheaper than, e.g., noble metals and having good catalytic performance. The structure and use of Perovskite-type mixed oxides has previously been thoroughly described and for more information we refer the reader to the literature [5, 6].

The combination of LSM and CGO is chosen as cathode material because LSM shows acceptable selectivity towards NO_x and CGO is chosen because of an acceptable oxide ion conductivity at exhaust gas temperatures [5]. Furthermore, K.K. Hansen et al has previously proven that this combination is able to catalyze the reduction of NO [5].

In order to obtain porous cathodes the presence of a pore former in the green specimen is necessary. This pore former should burn during sintering of the cathode and leave a pore behind. The use of graphite as pore former has previous been proved possible [7]. The use of high amounts graphite to the slurry is, however, undesirable as graphite has a relatively high level of impurities. For the graphite used in the study by K.B. Andersen et al the impurities were; Si 150 ppm, S 100 ppm, Fe 80 ppm, Ca 25 ppm, Al 20 ppm, Cr 5 ppm, Cu 5 ppm, Mo 3 ppm, Ni 3 ppm [specifications from supplier]. Thus a substituent with a lower level of impurities is preferable. Furthermore due to process conditions during tape casting the use of graphite as pore former will result in large pores orientated perpendicular to the air flow direction leading to a higher pressure drop over the final cathode so a higher load of pore former is needed to overcome the effect of perpendicularly orientated porosity and this will compromise the mechanical properties of the final electrochemical cell.

PMMA microparticles have a lower level of impurities and are due to their spherical shape not able to produce porosities perpendicular to the flow direction. PMMA microparticles have previously been proven promising in the preparation of porous materials for solid oxide fuel cells [8-11]. PMMA will, however, often result in closed porosity [12, 13]. For this reason a mixture of PMMA and graphite was tested as possible pore former. The hypothesis is that the graphite will interconnect the pores formed by the PMMA particles. This will reduce the overall level of impurities in the final electrochemical cells. In this study we investigate the effect of the size of PMMA pore formers on the linear micro structure and the porosity of the cathode layer for electrochemical cells. Furthermore linear shrinkage and the airflow through the cathode material were measured.

Experimental

Preparation of suspensions and tapes

The powders used in the present study were $(La_{0.85}Sr_{0.15})_{0.9}MnO_3$ (LSM15) from Haldor Topsoe A/S, Denmark calcined at 800 °C and 1200 °C respectively and $Ce_{0.9}Gd_{0.1}O_{1.95}$ (CGO) from Rhodia, France. Graphite was from Alfa Aesar and the polymethyl methacrylate (PMMA) microparticles were from Esprix Technologies (see **Tab. 1**). A 1:1 ratio of LSM calcined at 800 °C and LSM calcined at 1200 °C were mixed and suspended in an azeotropic mixture of methylethylketone and ethanol with polyvinylpyrrolidone (PVP) as dispersant. After ball milling for 3 days 19 wt% CGO and more PVP were added and the suspension was milled for additional 24 h. Then 11.2 wt% PMMA microparticles and 4.8 wt% graphite was added and the suspension was milled for 5 h. Characteristics of the tested PMMA particles are listed in Tab. 1. Finally a mixture of binder, plasticizer

and a release agent was added and the suspension was milled over night. The suspension was tape casted, using a doctor blade adjusted to 250 μm at a casting speed of 20 cm/min.

The composition of the prepared tapes can be found in Tab. 2. When the tapes were dry 8 layers of tape were laminated together by the method described by Larsen and Brodersen [14]. After lamination the samples were sintered at 1250 $^{\circ}\text{C}$ for 6 h.

Characterization

Particle size distribution (PSD) was measured after each step using a laser diffraction particle size analyzer (LS13320, Beckman Coulter, USA). The viscosity of the suspension was measured before tape casting using a Haake RheoStress 600 rheometer (Thermo-scientific, USA) with parallel plate configuration and 0.1 mm separation between the plates. The suspensions were adjusted to the desired viscosity prior to tape casting.

The shrinkage of the samples during sintering was characterized by measuring the change in dimensions upon sintering. The microstructure of the sintered samples was examined in Hitachi tabletop microscope (TM1000) and the porosities and the pore size distributions were characterized by mercury porosimetry (AutoPore IV, Micromeritics, USA).

Finally the air flow through the cell was measured according to the procedure described by K.B. Andersen et al [7]

Results and discussion

All the sintered samples were analyzed with scanning electron microscopy (SEM) and the SEM micrographs are shown in Fig. 1. All the prepared samples are porous, but a significant difference in average pore diameter is observed for the samples.

The measured shrinkage, porosity, average pore size and flow rate of air through the prepared cathodes are listed I Tab. 3.

All the tested pore formers resulted in porous cathodes and the porosities are ranging from 25.2 to 46.4 % open porosity. This proves that the graphite indeed is able to interconnect the PMMA induced porosities. The porosity observed in sample no. 5 is equal to the porosity of a sample prepared with just graphite as pore former in previously reported results (47.4 % porosity) [7]. This proves it possible to replace some of the graphite with PMMA microparticles.

Also the flow rate through the different cathodes is high and with less than 7 % difference between the highest and lowest value. Higher flow rates across the cathode is obtained for all the prepared cathodes comparing with the flow rate (5.31 ml/(min*mm²)) reported by K.B. Andersen on samples prepared with graphite. From these results it is concluded that the substitution of some of the graphite with PMMA microparticles increases the flow rate across the cathode and proves that the PMMA porosities are oriented more in line with the direction of the air flow comparing with the graphite induced porosities. That is because the graphite has a more rod like shape, that a lines in the casting direction, perpendicular to the flow direction.

To test the effect of solvent swelling of the pore former on the pore size the standard weight (16 wt.%) of MR10G was allowed to swell in MEKET for 4 days before addition to the slurry. This resulted in samples with a porosity of 36.9 % and average pore diameter of 0.64 μm . From this experiment it was concluded that time the pore former is suspended in solvent has an effect on the final pore size in the cathode. The pore size expected to increase as a result of swelling but instead the pore diameter decreased probably due to dissolution of the surface layer of the pore former. This result was confirmed with SEM (See **Fig. f**). It was also found that swelling of the pore former in MEKET resulted in a higher shrinkage (28.8 %) during sintering probably increased amounts of dissolved PMMA will mix with binder and in this way increase the shrinkage during sintering. From this experiment it was concluded that the highest porosity was obtained by minimizing the time the pore former is in contact with MEKET.

Also the effect of milling time was investigated. LSM was milled with PVP in MEKET for 8 days instead of the standard 3 days. This had a negative effect on the porosity and the porosity decreased from 46.4 % to 35.9 % and the average pore diameter decreased from 0.98 μm to 0.66 μm . This lowered porosity probably originates from a better packing of the LSM and CGO particles in the tape, which will result in a higher density of the fired specimen. These specimens showed a shrinkage of 29.7 %. A higher shrinkage than for the sample with LSM milled for 3 days and emphasizes the better packing of the particles.

Conclusion

It was found possible to prepare porous cathodes with use of a mixture of graphite and PMMA microparticles as pore former. From the present study it was concluded that addition of the pore former MR10G from Esprix resulted the most porous cathodes, which also had the highest measured air flow across the sample. It was also found that prolonged milling of the LSM had an effect on the porosity of the fired cathode probably due to better packing of the particles resulting in a higher density of the fired cathode and lower porosity.

The PMMA microparticles were dissolvable in MEKET and the time PMMA is in contact with MEKET should be minimized. From the SEM micrographs and porosity measurements a decreased pore diameter was observed. This decrease in diameter could originate from dissolution of the PMMA surface resulting in reduction of the pore former diameter and a reduced weight percent of PMMA microparticles as the dissolved PMMA will mix with the binder.

Acknowledgement

The Danish Research Council is thanked for financial support (contract no. 09-065186).

References

- [1] A.R. Butler, D.L.H. Williams, The Physiological-Role of Nitric-oxide, Chem. Soc. Rev., 22 (1993) 233
- [2] S.E. Manahan, Environmental chemistry, 6th edn. CRC, London (1994)
- [3] H. Muhle, *Toxic and Carcinogenic effects of fine particles – observations and hypotheses*. In: International ETH work-shop on nanoparticle measurement, Zürich: ETH, paper 2 (1999)

- [4] J. Dinesen, S.S. Nissen, H. Christensen, Electrochemical Diesel Particulate Filter, SAE paper no. 980547 (1998)
- [5] K.K. Hansen, E.M. Skou, H. Christensen, Perovskites as Cathodes for Nitric Oxide Reduction, *J. Electrochem. Soc.*, 147 (2000) 2007
- [6] J. Zhu, A. Thomas, Perovskite-type mixed oxides as catalytic material for NO removal, *Applied Catalysis B-Environmental*, 92 (2009) 225
- [7] K.B. Andersen, F.B. Nygaard, Z. He, M. Menon. K.K. Hansen, Optimizing the performance of Porous Electrochemical Cells for Flue Gas Purification using the DOE method, *Ceram. Int.* 37 (2011) 903
- [8] J.C. Ruiz-Morales, J. Canales-Vazquez, J. Pena-Martinez, D. Marrero-Lopez, Microstructural optimisation of materials for SOFC applications using PMMA microspheres, *J. Mat. Chem.*, 16 (2006) 540
- [9] L. Mingyi, Y. Bo, X. Jingming, J. Chen, Influence of pore formers on physical properties and microstructures of supporting cathodes of solid oxide electrolysis cells, *Int. J. Hydrogen Energy*. 35 (2010) 2670
- [10] D. Marrero-Lopez, J.C. Ruiz-Morales, J. Pena-Martinez, J. Canales-Vazquez, P. Nunez, Preparation of thin layer materials with macroporous microstructure for SOFC applications, *J. Solid State Chem.*, 181 (2008) 685
- [11] J.C. Ruiz-Morales, J. Canales-Vazquez, J. Pena-Martinez, D. Marrero-Lopez, P. Nunez, On the simultaneous use of $\text{La}_{0.75}\text{Sr}_{0.25}\text{Cr}_{0.5}\text{Mn}_{0.5}\text{O}_{3-\delta}$ as both anode and cathode material with improved microstructure in solid oxide fuel cells, *Electrochim. Acta*, 52 (2006) 278
- [12] M. Descamps, T. Duhoo, F. Monchau, J. Lu, P. Hardouin, J.C. Hornez, A. Leriche, Manufacture of macroporous beta-tricalcium phosphate bioceramics, *J. Euro. Ceram. Soc.*, 28 (2008) 149
- [13] H.S. Cruz, J. Spino, G. Grathwohl, Nanocrystalline ZrO_2 ceramics with idealized macropores, *J. Eur. Ceram. Soc.*, 28 (2008) 1783
- [14] P.H. Larsen, K. Brodersen, K. Beurodereusen, P.H. Rareusen, US2008124602-A1; JP2008130568-A; EP1930974-A1; CN101242003-A; CA2611362-A1; KR2008047282-A; KR966845-B1, (2008)

Figure Captions

Fig 1. SEM micrographs of the sintered specimens. a) Sample no. 1, b) sample no. 2, c) sample no. 3, d) sample no. 4, e) sample no. 5, f) sample no. 6 and g) sample no. 7.

Table titles

Tab. 1 Characteristics of the tested PMMA pore formers (specifications from supplier)

Tab. 2 Composition of the prepared samples

Tab. 3 Characteristics of the sintered tapes

Figures

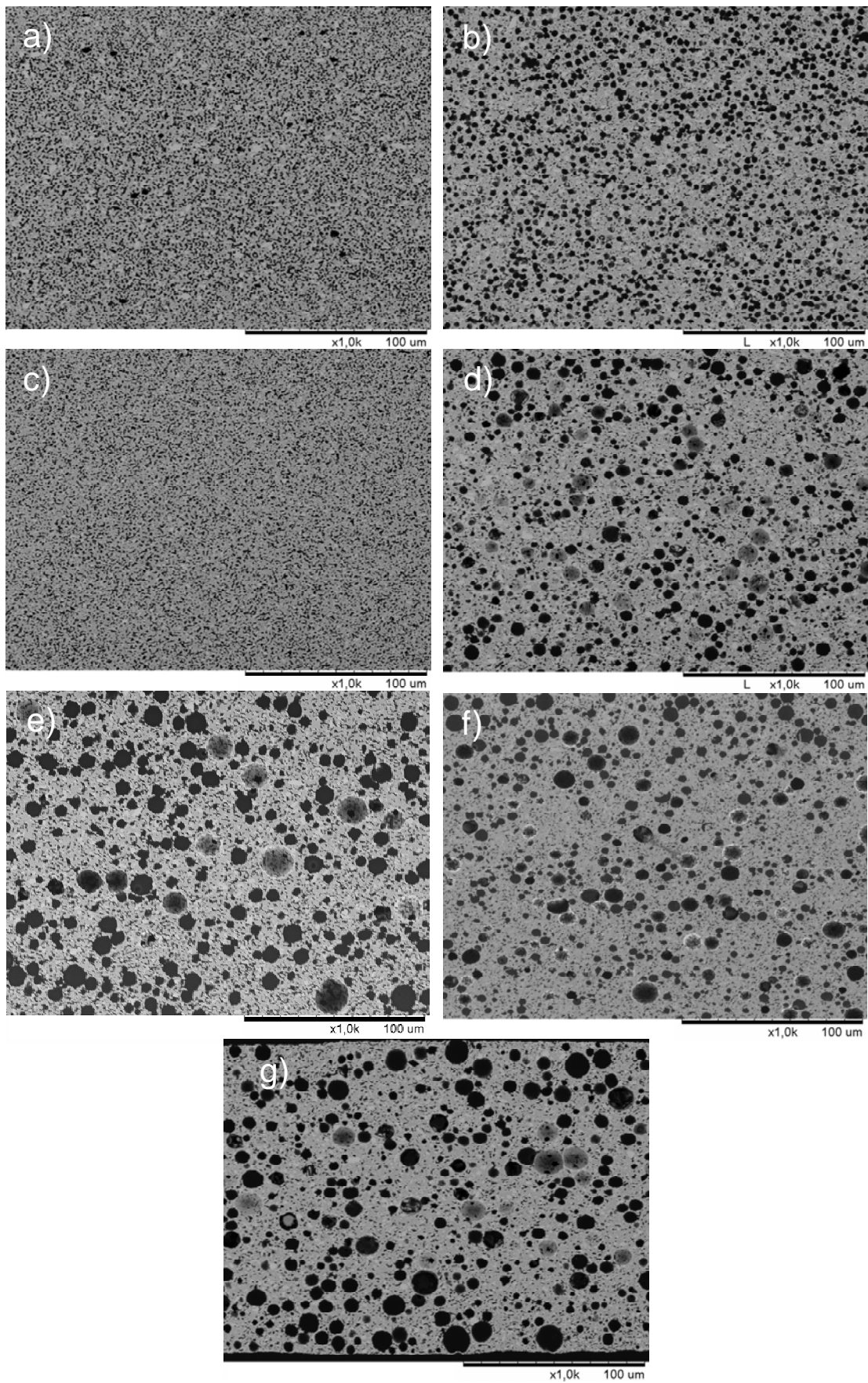


Fig. 1 SEM micrographs of the sintered specimens. a) Sample no. 1, b) sample no. 2, c) sample no. 3, d) sample no. 4, e) sample no. 5, f) sample no. 6 and g) sample no. 7.

Tables

Tab. 1 Characteristics of the tested PMMA pore formers (specifications from supplier)

PMMA	Particle size (μm)	Monodisperse
MX180	1.8 ± 0.20	Yes
MX500	5 ± 0.50	Yes
MR2G	2	No
MR7G	5	No
MR10G	9	No

Tab. 2 Composition of the prepared samples

Sample	Composition
1	LSM-CGO with 11.2 wt.% MX180
2	LSM-CGO with 11.2 wt.% MX500
3	LSM-CGO with 11.2 wt.% MR2G
4	LSM-CGO with 11.2 wt.% MR7G
5	LSM-CGO with 11.2 wt.% MR10G
6	LSM-CGO with 11.2 wt.% MR10G*
7	LSM-CGO with 11.2 wt.% MR10G**

*MR10G was allowed to swell in MEKET 4 days before addition

** LSM milled for additionally 5 days

Tab. 3 Characteristics of the sintered tapes

Sample	Shrinkage (%)	Porosity (%)	Pore size (μm)	Flow rate ($\text{ml}/(\text{min} \cdot \text{mm}^2)$)
1	31.9	32.9	0.59	5.55
2	29.9	37.0	0.72	5.49
3	31.9	25.2	0.52	5.39
4	29.3	37.9	0.69	5.50
5	24.2	46.4	0.98	5.77
6	28.8	36.9	0.64	5.31
7	29.7	35.9	0.66	5.40